

Engineering Research Express



PAPER

Portable universal tensile testing machine for studying mechanical properties of superelastic biomaterials

RECEIVED
13 October 2021

REVISED
29 November 2021

ACCEPTED FOR PUBLICATION
9 December 2021

PUBLISHED
22 December 2021

Sergey V Gunter¹, Ekaterina S Marchenko¹, Yuriy F Yashenchuk¹, Gulsharat A Baigonakova¹ and Alex A Volinsky^{1,2} 

¹ National Research Tomsk State University, 36 Lenin Ave., Tomsk 634050, Russia

² Department of Mechanical Engineering, University of South Florida, 4202 E. Fowler Ave. ENG030, Tampa 33620, United States of America

E-mail: volinsky@usf.edu

Keywords: universal tensile testing machine, compact design, uniaxial tension, low modulus materials, superelastic materials, NiTi

Abstract

A portable universal tensile testing machine for single and cyclic loading of superelastic biomaterials is presented. It's an alternative to large-sized stationary universal testing machines. The machine is designed to obtain uniaxial cyclic tension stress-strain curves of materials with a low elastic modulus, including biological tissues. Its portability allows using it in various conditions: classrooms, production laboratories, and in the field. An interface has been developed to connect it to a computer. Computer output of experimental data allows recording and displaying load-displacement curves, setting the number of cycles, limits, and rate of cyclic deformation. Several examples of testing various biomaterials are presented. The functional advantage of the device is the wide tensile testing speed range of $0.01\text{--}10\text{ mm s}^{-1}$ and cyclic loading, which allow capturing viscoelastic and superelastic behavior of biomaterials.

1. Introduction

When developing biological implants made from nitinol (NiTi), there is a challenge of characterizing their viscoelastic properties, stress hysteresis, and delayed unloading deformation under cyclic tension [1–5]. Nitinol is a biocompatible material that has high physical and mechanical properties, while exhibiting shape memory effects and superelasticity. Superelastic NiTi materials exhibit adequate biocompatibility paired with high cyclic deformation without accumulation of permanent strain and loss of mechanical strength [6–8]. To characterize the mechanical properties of thin wires and knitted meshes made from NiTi alloys, measuring equipment is required to accurately capture the superelastic behavior of the material during monotonic and cyclic tests at different tensile strain rates [9–11]. At the same time, the hardware must meet modern digital control requirements with the ability to display data in real-time during the test, along with saving and processing obtained data [12–17].

There are several devices available for studying the deformation behavior of superelastic materials, ranging from simple mechanical devices to automated computerized machines. Devices for cyclic tensile loading of fibers contain a large number of kinematic joints and nodes, which reduce measurement accuracy, and sometimes lack digital control and data processing [18–20]. At the same time, there are computerized universal testing machines manufactured by Instron (USA), MTS Systems (USA), and Testex (China) [21–28]. These machines have a rigid frame with vertical guides, along which the traverse is moved by a motor. The sample is secured in the grips, one of which is fixed, and the other is attached to the traverse.

Existing large-sized universal testing machines are stationary: floor-standing or table-top. Of the least bulky installations, we mention the C41 machine from the Criterion catalog, which develops a force up to 10 kN, with a mass of 60 kg and a height of 2 m [20]. A similar device TB400 from Testex, weighing about 100 kg, is used to measure the fiber strength [25]. However, this device is not suitable for cyclic loading. The closest device with similar functionality to the presented design is the Instron 3340 universal testing machine, which has the option

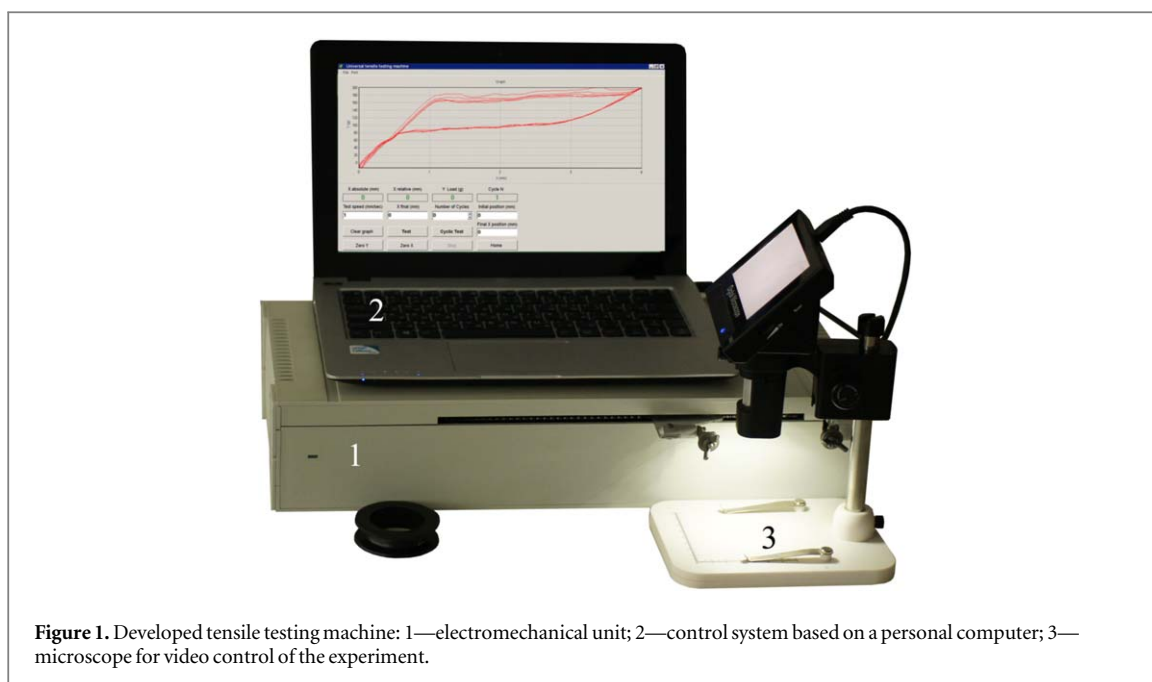


Figure 1. Developed tensile testing machine: 1—electromechanical unit; 2—control system based on a personal computer; 3—microscope for video control of the experiment.

of cyclic measurements [28]. The device contains electromechanical and electronic parts. The electromechanical part consists of a base on which guides with movable and fixed traverses are fixed, a power drive, power supply units, a movable traverse, load and displacement sensors, and clamps for fixing the samples. The electronic part includes a control unit. The 38 kg device's maximum load is 500 N with $\pm 0.5\%$ accuracy, and $\pm 20 \mu\text{m}$ strain resolution (0.15%). This machine is bulky and requires stationary installation. The Instron 5582 universal testing machine is also analogous to the developed device [25]. This stationary unit has a vertical frame. The machine has the option of testing samples in a temperature chamber from -100°C to 320°C . The strain rate is in the $0.00001\text{--}8 \text{ mm s}^{-1}$ range with a $2\text{--}100,000 \text{ N}$ load range. The software does not allow modifying or reconfiguring the control system.

The closest analog with a horizontal stepper motor as an actuating mechanism is a mobile testing machine [12], which has a similar layout of the main blocks in combination with a ball screw drive located in the same horizontal plane as the sample. The deformation of the sample is realized according to a similar scheme, where one end of the sample is fixed in a movable grip, and the other is fixed in a grip with a built-in force transducer. The electromechanical unit is located in one housing, and the test speed ranges from 0.001 mm s^{-1} to 1 mm s^{-1} with the possibility of testing samples up to 50 mm long with a 20 mm maximum travel distance. The device does not allow testing samples in a cyclic mode. The interface is coordinated through the LabVIEW software package, and the platform is designed as a virtual instrument in a graphical format. The analysis of the existing testing devices suggests that the development of a universal uniaxial tensile testing machine with combined mobility, compactness, and optimized measurement accuracy, and a convenient interface is needed for testing superelastic biomaterials.

2. Developed portable device

The presented machine is controlled through a USB interface, which can be connected to a computer using the 'Line_Tester' application (figure 1). The majority of the machine parts are commercially available, including the stock housing made of plastic, making it less expensive than the commercial analogs. When comparing the capabilities of the developed machine and the universal testing machine Instron 68T-5 [29], it's important to make sure that their capabilities are comparable and sufficient for certain tasks (table 1). The developed device has a lower accuracy of positioning, stress, and strain measurements compared with stationary commercial machines. However, the accuracy of traverse positioning, movement, and sample strain control allows detecting and recording all the features of the deformation behavior of fiber superelastic biological tissues, elastomers, and alloys. The developed universal machine is capable of testing small-sized samples made from low-modulus and tensile strength materials with the corresponding developed forces up to 200 N and a relative elongation of 1%–200%. The device allows conducting experiments in the field and laboratory conditions with the possibility of direct demonstration through a projector or remotely through the internet. The machine design allows video recording of the sample during the test for further processing, including thermal imaging and digital image

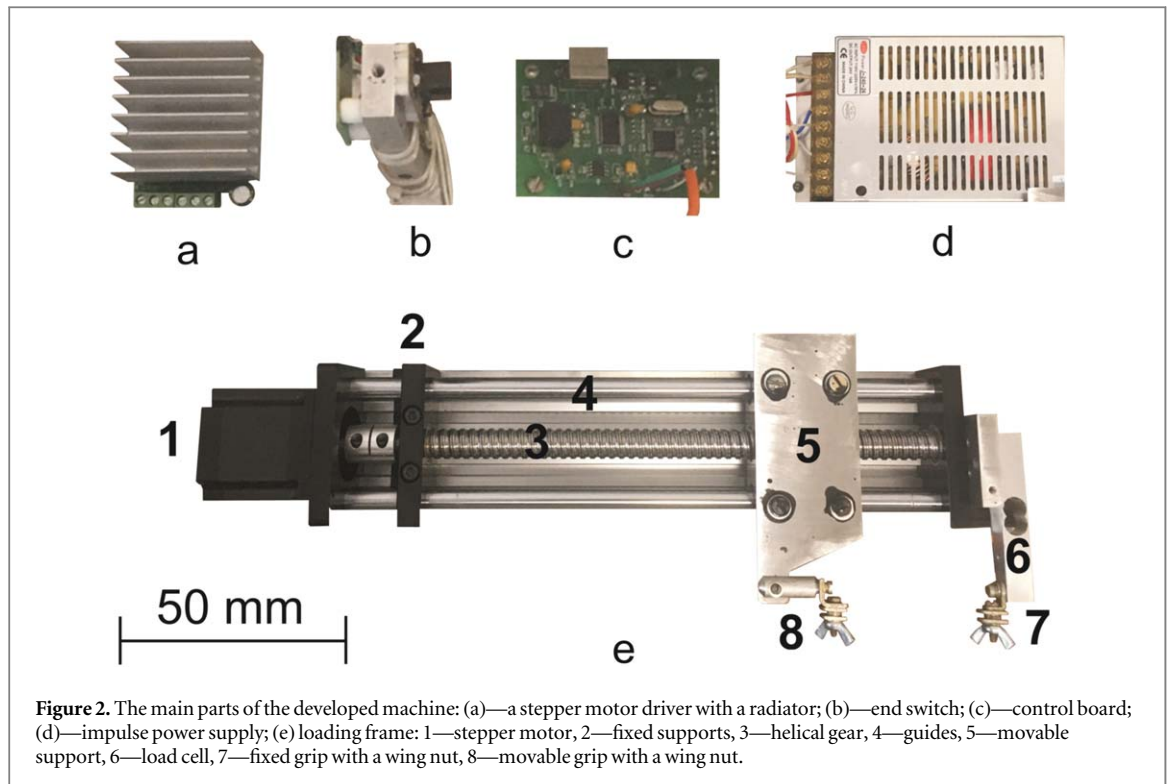


Figure 2. The main parts of the developed machine: (a)—a stepper motor driver with a radiator; (b)—end switch; (c)—control board; (d)—impulse power supply; (e) loading frame: 1—stepper motor, 2—fixed supports, 3—helical gear, 4—guides, 5—movable support, 6—load cell, 7—fixed grip with a wing nut, 8—movable grip with a wing nut.

Table 1. Portable universal testing machine characteristics compared with Instron 68T-5.

Parameter	Developed machine	Instron 68T-5
Maximum traverse travel distance	300 mm	420 mm
Traverse positioning accuracy	0.15 μm	0.0095 μm
Displacement resolution	$\pm 0.1 \mu\text{m}$	$\pm 0.05 \mu\text{m}$
Test speed	0.01–10 mm s^{-1}	0.0015–50 mm s^{-1}
Maximum load	200 N	5,000 N
Maximum number of tensile cycles	1,000	—
Test area width	250 mm	420 mm
Weight of the device	5 kg	62 kg

correlation for more accurate strain determination and data analysis. Other options can be developed, including testing samples in liquids.

The main part of the developed tensile machine is an electromechanical unit with an electronic drive control block. The combined arrangement of the guides, the movable cross-beam, the load cell, the drive, and the drive control unit in a single housing ensures the compactness of the machine. The electromechanical unit was selected based on the machine operational requirements (figure 2). The developed tensile testing machine consists of the following main components: control board (CP); load measurement board (LMB); servo stepper motor (SSM); strain gauge (SG); end switches (ES); and power supply (PS). The bridged resistive strain gauge is optimally designed and sized for integration into the device. The strain gauge was chosen according to required sensitivity, nominal and maximum load, and overall dimensions. The sensor is used to measure the developed forces and is mounted on a fixed traverse. Coordination of the sensor indications with the control board provides control of a stepper motor (SM) through a driver (SMD). The applied load is measured through the load sensing board (LSB).

The control of the end positions of the movable traverse is carried out by the ESs. Data exchange with a personal computer (PC) is realized via a USB interface. The control panel includes a 32-bit microcontroller with an ARM Cortex core, which generates control signals for the SMD. The microcontroller performs mathematical calculations and processing of the received data from the SG and ES, followed by sending the results to the PC. The USB interface driver serves as an intermediary between the PC and the microcontroller. The load sensing board converts the analog data from the load cell into digital values. The LMB includes an analog-to-digital converter and provides a voltage reference. Data from the LMB to the control panel are transmitted via a serial port at a frequency of 10 Hz. The SMD is powered by a $\pm 24 \text{ V}$ switching power supply. Control signals are

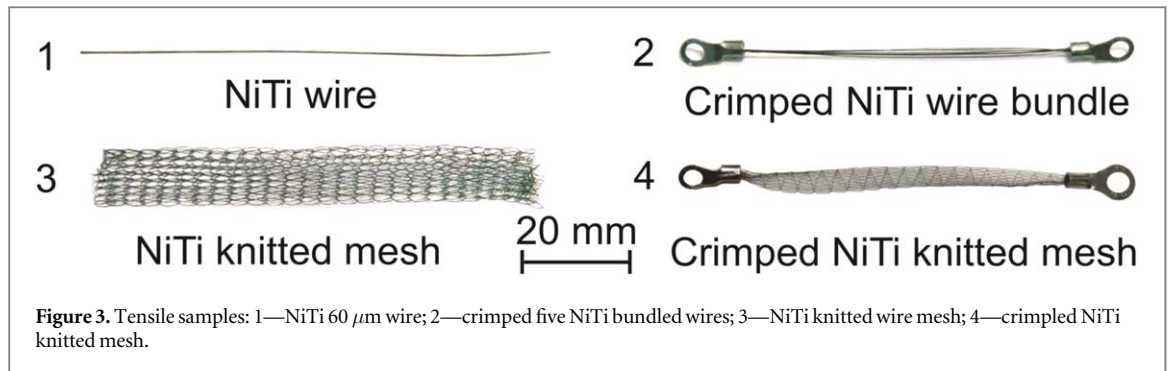


Figure 3. Tensile samples: 1—NiTi 60 μm wire; 2—crimped five NiTi bundled wires; 3—NiTi knitted wire mesh; 4—crimped NiTi knitted mesh.

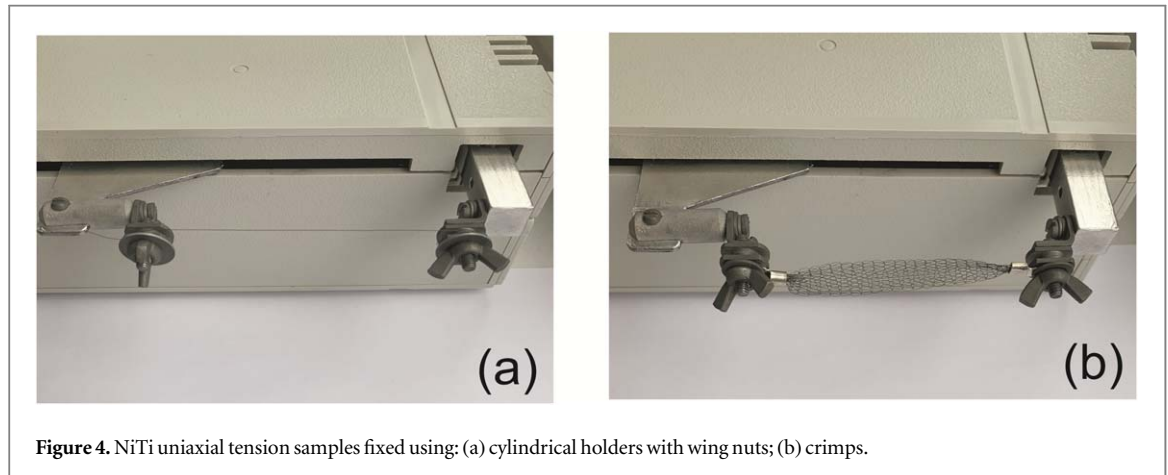


Figure 4. NiTi uniaxial tension samples fixed using: (a) cylindrical holders with wing nuts; (b) crimps.

generated by the computer interface and fed to the SMD through the CP, which sets the speed and direction of the traverse movement. The accuracy of the stepper motor positioning is determined by its rotation. SMD divides the standard SM into smaller steps, thereby increasing the positioning accuracy.

The horizontal arrangement of the guides and the movable traverse reduces the height of the device and allows optimizing its dimensions to achieve a compact layout. The high-precision helical gear has a positioning accuracy on the order of 1–3 μm . Cyclic measurements require adequate repeatability; therefore, the positioning accuracy of the traverse is important. The 1.8 degrees two-phase stepper motor used in the developed device has 200 full steps per revolution. The 200 full steps of the SM with 1/16 step precision results in 3,200 micro-steps of the traverse movement per full revolution of the stepper motor. The helical gear has a 5 mm lateral movement per revolution (pitch), providing the traverse positioning accuracy of 1–3 μm , which corresponds to about 0.01% strain resolution for a 30 mm long sample. Thus, further reduction of the pitch is not necessary in this case.

The load capacity of the tensile machine is determined by the load cell characteristics. The maximum load cell capacity in the developed machine is 200 N, which is adequate for testing superelastic biomaterials. The load cell sensitivity is 0.1 g at the 10 Hz data collection rate. When the traverse moves at 1 mm s^{-1} , 640 stepper motor pulses are required, 0.1 mm s^{-1} speed requires 64 pulses, and 0.01 mm s^{-1} requires 6 pulses, respectively. The relative strain error is proportional to the absolute strain, for example, it is 0.067% for 1 mm absolute strain, 0.67% for 10 mm absolute strain, and 6.67% for 100 mm absolute strain, respectively. Even though the developed machine is universal, the load cell is fixed to guarantee fixed frame compliance. This approach also makes it less expensive. Technically, the load cell can be changed, but this needs to be reflected by the proper calibration and software modifications.

Positioning of the traverse, reading, transmission, and processing of the data occurs simultaneously, therefore, the 38,400 bit s^{-1} USB port data transfer rate is adequate and does not affect the positioning accuracy of the traverse. The data transfer rate does not affect the overall operation of the device, since the frequency of the analog-to-digital data conversion rate is 10 Hz.

3. Preparing the device for operation

This device allows testing low modulus and superelastic materials, including thin and ultra-thin wire samples and biological tissues in single and cyclic loading modes. Implants differentiation according to rheological

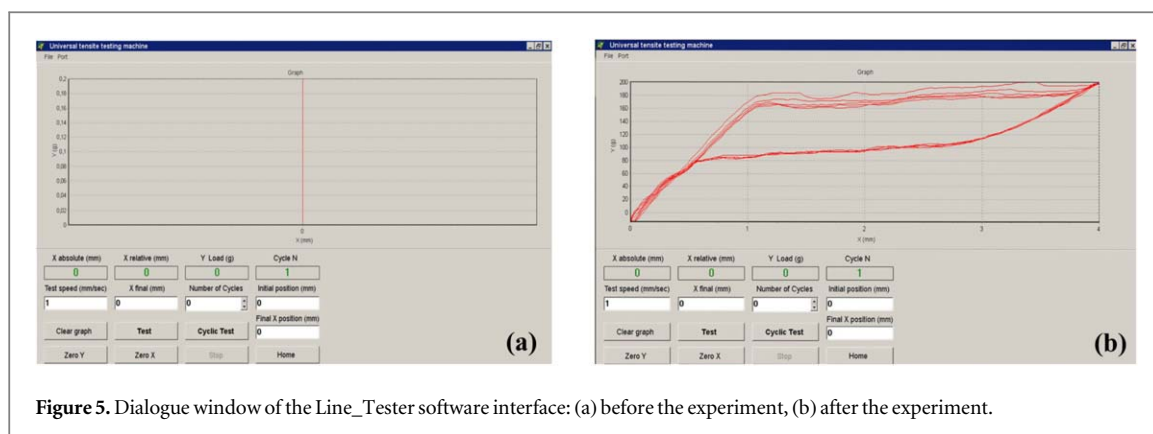


Figure 5. Dialogue window of the Line_Tester software interface: (a) before the experiment, (b) after the experiment.

correspondence is an important factor in the proper selection of the physical and mechanical properties of the implants and during their further interaction with biological tissues in service. In the long term, the risk of subjective errors is decreased when using materials with improved ‘implant-biological tissue’ biointerface [30]. The functional advantage of the device, when compared with analogs, is the wider speed range of $0.01\text{--}10\text{ mm s}^{-1}$. This allows capturing the viscoelastic behavior of bone and porous metal samples since at tensile testing speeds over 0.1 mm s^{-1} , this phenomenon is not observed. At the same time, the machine allows testing samples in a cyclic mode, up to 1,000 cycles.

Special cylindrical clamps are used for the wire samples, where the wire is first wound over the cylindrical holder before it is secured with a screw, eliminating the stress concentration at the clamping points of the sample holder. The portability of the device is an alternative solution to large-sized stationary machines, allowing research in the field. The simple design of the mechanical grips prevents stress concentration and premature failure of the samples. It allows testing fiber and wire samples without additional sample preparation. In this case, the wire sample is wrapped twice around the cylinder sleeve and fixed on the lateral outer side with a washer and a threaded wing nut. This method does not require extra wire sample preparation (figures 3 and 4).

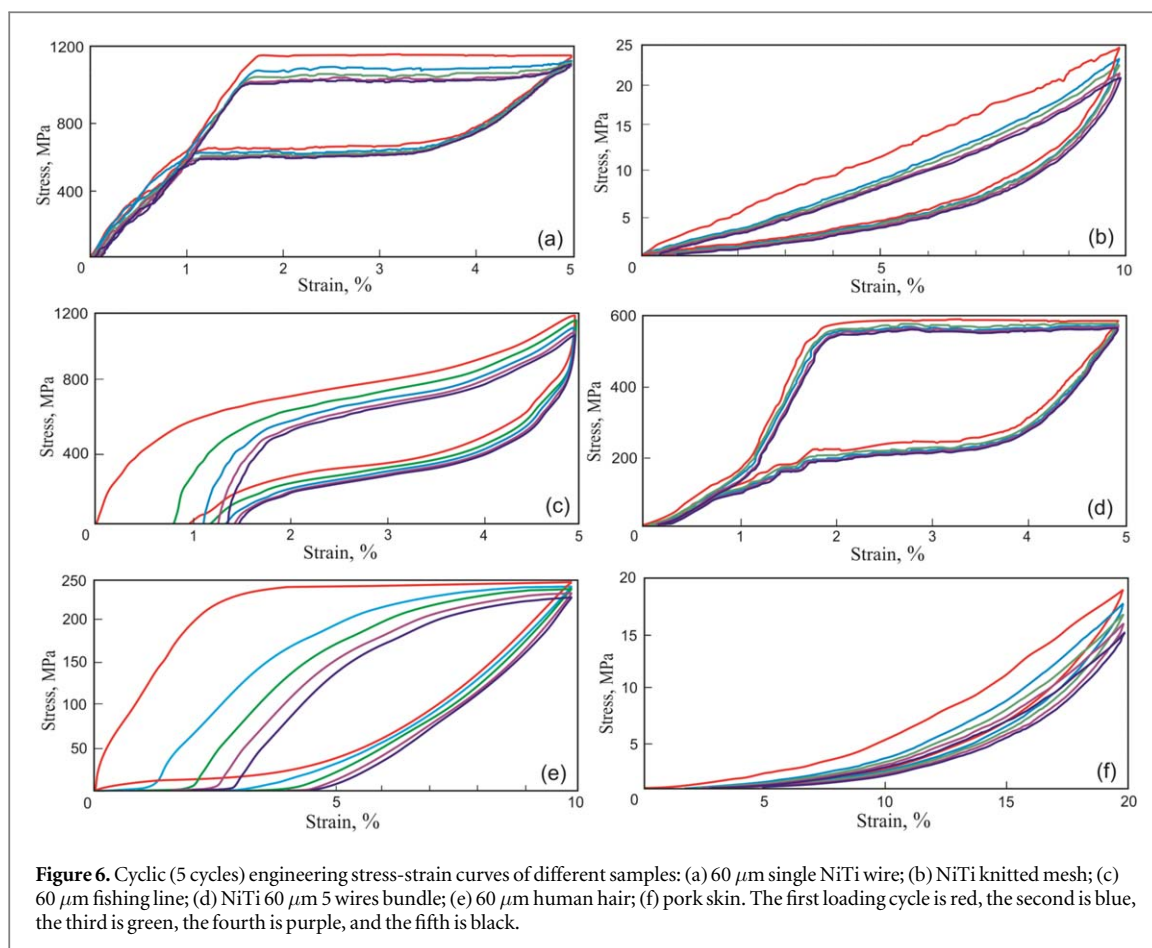
For the small-sized hard-to-fix samples of bones and other materials, it is preferred to secure the sample ends into universal crimp terminals using a hand crimping tool. In this case, the crimps are fixed on the grippers with washers and threaded wing nuts. The proper fixation of samples in the grips affects the measurement accuracy [27, 28]. Similar grips are used in other universal testing machines [18, 21–23]. Two types of fixing the samples are presented in figure 4.

The fracture of the sample does not occur at the grips, but rather in the middle between the grips, therefore, this method of attaching the samples is reliable. Crimps do not affect the obtained results. The method of crimping samples with the use of additional fixing inserts creates a fairly reliable connection. To do this, the ends of the sample are wrapped around with plastic material, for example, copper wire. Then the end of the sample together with the clip is crimped, avoiding the destruction of the sample material. For each sample, a pre-selected individual compression force is applied, since the strength of the samples is significantly different. The grips can be changed to accommodate different types of samples.

The developed universal tensile testing machine is controlled through the USB interface by using the Line_Tester software written for Windows operating system. The software interface displays the load-displacement curves up to 1,000 loading-unloading cycles in real-time with the ability to save the data in both graphical (BMP) and text (TXT) formats. The interface dialogue window allows setting the necessary parameters of monotonic and/or cyclic tension: strain rate, strain range, and the number of cycles in figure 5(a). The test can be stopped at any time with the ability to reset all testing parameters, returning the grips into their original position. The example in figure 5(b) shows the load-displacement curves of the cyclic tension of the $60\text{ }\mu\text{m}$ NiTi wire deformed up to 5% strain.

The developed universal tensile testing machine also has a portable microscope for visual control and assessment of the sample deformation uniformity during the tensile test. The microscope transmits a live video through a USB port to a PC in real-time during the test. This allows controlling the sample stretching process in real-time, along with recording the video for further processing, including the possibility of using digital image correlation for strain measurements in suitable samples.

The horizontal sample allows using the microscope on a standard stand without additional brackets or consoles, opposite to vertical stationary universal tensile testing machines [16, 21, 26]. This sample arrangement allows maintaining the device’s compactness, versatility, and portability. The prolonged usage experience of the developed universal tensile testing machine demonstrated components synergy and reliability, along with the repeatable test results. The test data are saved in both graphical and text formats for further processing.



4. Experimental data

Operating experience has shown that the device successfully detects all the features of the deformation behavior of superelastic and low-modulus materials. The stress-strain curves of NiTi alloys prove that the device is capable of capturing all features of tensile superelastic deformation.

The obtained stress-strain curves of various materials have individual characteristics captured in figure 6(a)–(f). The engineering stress-strain curves of NiTi wire have characteristic features of superelastic alloys: elastic and viscous deformation regions during loading; decrease in yield strength caused by phase hardening and non-linear softening during cyclic unloading; curves overlap during cyclic elastic and superelasticity loading and unloading regions in figure 6(a).

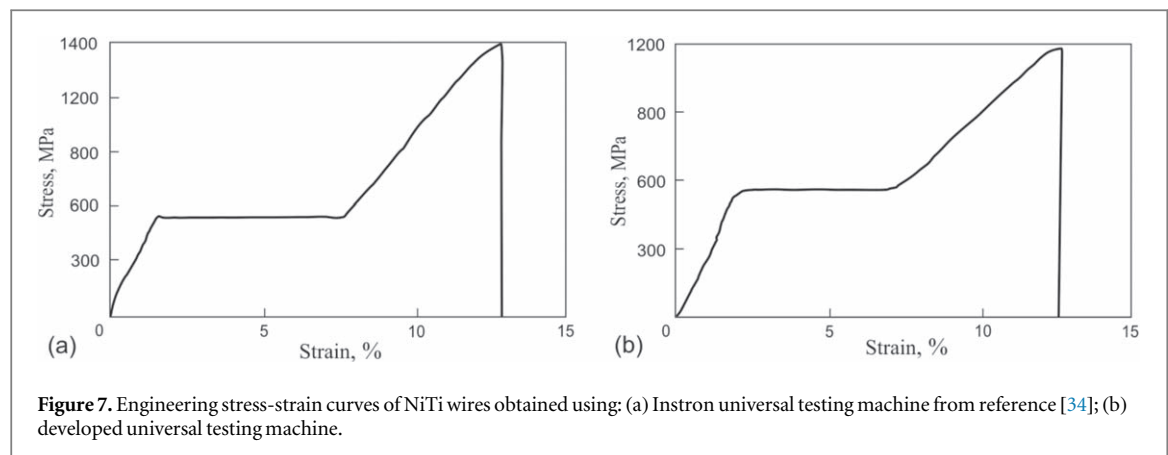
Engineering stress-strain curves from a bundle of 5 NiTi wires are similar to single wire results in figure 6(d), with the only difference being the yield stress. The stress-strain curves from NiTi mesh in figure 6(b) are similar to skin in figure 6(f). The softening effect was observed, which depends on the strain levels and the number of loading-unloading cycles. Each set of experiments consisted of testing 5 or more samples.

Viscoelastic stress-strain curves of 60 μm fishing line exhibited typical superelastic materials and polymer films behavior in figure 6(c) [31–33], where an increase in residual strain during cyclic loading was found. A 60 μm human hair was also tested. The stress-strain curves from a hair are similar to the 60 μm NiTi wire in figure 6(e), exhibiting pronounced elastic and viscoelastic regions. An increase in residual strain during cycling and hardening under load were observed.

Typically, 5 loading-unloading cycles were carried out at 0.1 mm s^{-1} test speed. Samples of different lengths, ranging from 20 mm to 180 mm, can be tested. The software interface allows setting the initial and final sample length and the test speed in the 0.01–10 mm s^{-1} range.

The obtained NiTi wire tensile data were experimentally compared with the literature data from commercial stationary installations (Instron). Machine compliance has been measured using a structurally rigid connection, demonstrating a linear transducer response up to a 200 N load. As a result, the elastic modulus data obtained using the device matched the known data, and the data measured using the commercial universal testing machine.

The device software controls, displays, and records the load in grams and the absolute strain in mm, and the data are saved in a text file. The device functionality is similar to its stationary counterparts. The sample load-



displacement curves are visualized and recorded in real-time. The instrument precision and design allow capturing all parts of the stress-strain curves of superelastic and biomedical materials.

NiTi wire deformation behavior obtained using Instron 3369 in figure 7(a) from the reference [34] is comparable with the developed device in figure 7(b). The engineering stress-strain curves transition from elastic deformation to a martensitic plateau (superelasticity) and then to irreversible deformation until rupture. Similarities of NiTi wire superelastic stress-strain curves obtained from Instron 3369 and the developed tensile testing machine suggest its correct operation. Using the NiTi wire stress-strain curves as an example, the measurement accuracy can be evaluated by comparison with published NiTi wire results obtained using Instron universal testing machine in figure 7(a), (b) [21, 34–37].

5. Conclusions

The developed universal tensile testing machine is an economic tool with all the necessary functionality of modern stationary universal tensile testing machines. The machine allows uniaxial cyclic tension testing and obtaining load-displacement diagrams of low-modulus superelastic materials, including biological tissues, elastomers, and alloys. The developed machine can test various samples at constant strain rates with a maximum load of 200 N and up to 1,000 cycles. The main features of the machine include a wide strain rate, compactness and mobility, which distinguish it from other stationary commercial instruments. The minimum strain rate can be set low enough to detect structural rearrangement processes in polymeric materials along with martensitic transformations in shape memory alloys. The machine is capable of testing thin wires and fibers.

Acknowledgments

This research was supported by the Ministry of Education and Science of the Russian Federation (Grant 0721-2020-0022).

Data availability statement

All data that support the findings of this study are included within the article (and any supplementary files).

ORCID iDs

Alex A Volinsky  <https://orcid.org/0000-0002-8520-6248>

References

- [1] Henderson E, Nash D and Demster W 2011 On the experimental testing of fine Nitinol wires for medical devices *J. Mech. Behav. Biomed.* **4** 261–8
- [2] Lavakuma A 2017 Mechanical properties of materials *Cons. Physical. Metallurgy* **5** 5–22
- [3] Wang C, Xiang X, Yao P, Paul Le F, Julien M and Zhigang S 2019 Elastic materials with high strength and low hysteresis *PNAS* **116** 5967–72
- [4] Huerta E, Corona J and Oliva A 2010 universal testing machine for mechanical properties of thin materials *Rev. Mex. Fis.* **56** 317–22

- [5] Kondratov A and Zachinjaev G 2015 Thermal cyclic tests of shrink polymeric product with the shape memory *Testing and Measurement. Techniques and Applications in Proc. of the 2015 Int. Conf. on Testing and Measurement: Techniques and Applications* 73–6
- [6] Gunther V, Radkevich A, Kang S-B, Marchenko E and Gyunter S 2019 Study of the knitted TiNi mesh graft in a rabbit cranioplasty model *Biomed. Phys. Eng. Express* **5** 1–12
- [7] Shtin V, Novikov V, Chekalkin T, Gunther V, Marchenko E, Chojnzonov E, Kang J-H, Chang M J, Kang S-B and Obrosova A 2019 Repair of orbital post-traumatic wall defects by custom-made TiNi mesh endografts *J. Funct. Biomater.* **10** 154–165
- [8] Gyunter V, Marchenko E, Gyunter S and Baigonakova G 2018 The influence of the surface layer on the combination of properties of thin TiNi alloy wires *Tech. Phys. Lett.* **44** 811–3
- [9] Leineweber M 2020 Take-home tensile testing system for biomechanics education *Biophysicist* **1** 36–44
- [10] Yadav S and Ganswar S 2018 An overview on recent progresses and future perspective of biomaterials *Mat. Sci. Eng.* **404** 81–89
- [11] Chang Y, Wang B, Li X, Wang C, Zhao M and Dong H 2019 A new continuous tensile-compressive testing device with friction-counteracting and anti-buckling supporting mechanism for large strain *J. Mater. Process. Tech.* **278** 813–846
- [12] Lim W and Kim H-K 2013 Design and development of a miniaturised tensile testing machine *G. J. Eng. Educ.* **15** 48–53
- [13] Bergonzi L, Vetteo M and Pironi A 2019 Development of a miniaturized specimen to perform uniaxial tensile tests on high performance materials *Proc. Struct. Integr.* **24** 213–24
- [14] Zhang S, Rauniyar S, Shrestha S and Ward A 2019 An experimental study of tensile property variability in selective laser melting *J. Manuf. Process.* **43** 26–35
- [15] Bamberg E, Grippo C, Wanakamol P and Slocum A 2006 A tensile test device for *in situ* atomic force microscope mechanical testing *Precis. Eng.* **30** 71–84
- [16] Liu X and Lu R 2020 Testing system for the mechanical properties of small-scale specimens based on 3D microscopic digital image correlation *Sensors* **20** 1–21
- [17] Zhong J and He D 2015 Combination of universal mechanical testing machine with atomic force microscope for materials research *Sci. Rep.* **5** 72–87
- [18] Pieczyska E, Tobushi H, Takeda K and Stroz D 2012 Martensite transformation bands studied in TiNi shape memory alloy by infrared and acoustic emission techniques *Metallic Materials* **50** 309–18
- [19] Matsui R, Takeda K and Tobushi H 2017 Mechanical properties of shape memory alloys and polymers a review on the study. Advances in shape memory materials *Advanced Structured Materials.* **73** 93–114
- [20] Klesa J, Plaset V, Foltete E and Collet M 2009 Experimental evaluation of the rheological properties of veriflex shape memory polymer ESOMAT. *Prague* **04006** 1–7
- [21] Frost M, Jury A, Heller L and Sedlak P 2021 Experimentally validated constitutive model for NiTi-based shape memory alloys featuring intermediate R-phase transformation: a case study of Ni₄₈Ti₄₉Fe₃ *Mater. Des.* **203** 1–13
- [22] Pieczyska E, Gadaj S, Nowacki W and Tobushi H 2006 Phase-transformation fronts evolution for stress- and strain-controlled tension tests in TiNi shape memory alloy *Exp. Mech.* **46** 531–42
- [23] Dunic V, Pieczyska E, Kowalewski Z and Matsui R 2019 Experimental and numerical investigation of mechanical and thermal effects in TiNi SMA during transformation-induced creep phenomena *Materials.* **12** 883
- [24] Kim J and Reda Taha M 2014 Experimental and numerical evaluation of direct tension test for cylindrical concrete specimens *Advances in Civil Engineering* **8** 156926
- [25] Anggraini N, Hasratiningsih Z and Subrata G 2010 Composition, tensile strength, and elastic modulus of Orden as cast post alloy *Padjadjaran Journal of Dentistry.* **22** 2–10
- [26] Zhang Y, Cheng X and Cai H 2016 Fabrication, characterization and tensile property of a novel Ti₂Ni/TiNi micro-laminated composite *Mater. Des.* **92** 486–93
- [27] Pieczyska E, Tobushi H and Kulasinski K 2013 Development of transformation bands in TiNi SMA for various stress and strain rates studied by a fast and sensitive infrared camera *Smart Mater. Struct.* **22** 183–191
- [28] Thornton J, Allen S and Arnett S 2000 *Effect of Gripping Technique on Tensile, Tensile Creep and Tensile Creep-Rupture Results for a High Tenacity Polyester Yarn in Grips, Clamps, Clamping Techniques, and Strain Measurement for Testing of Geosynthetics.* (West Conshohocken, PA: ASTM International) 47–67
- [29] Kondratov A and Benda A 2018 Relaxation processes in the shrinkable polyvinylchloride films with tactile marking of shrinkable labels *Chemist. Physic. of Eng. Mat. Waretown.* **4** 179–188
- [30] Yashchuk Y, Marchenko E, Gunter S, Baiganakova G, Kokorev O and Volinsky A A 2021 Softening effects in biological tissues and NiTi knitwear during cyclic loading *Materials* **14** 6256
- [31] Kondratov A, Zueva A, Varakin R, Taranec I and Savenkova I 2018 Polymer film strain gauges for measuring large elongations *Polymer film strain gauges for measuring large elongations in IOP Conf. Series Materials Science and Engineering. Workshop on Materials and Engineering in Aeronautics* 312(15-16 November 2017)
- [32] Kondratov A, Konovalova M, Cherkasov E and Savenkova I 2017 Non-destructive assessment of relief marking parameters of heat shrinkable installation parts for aviation technology *MATEC Web of Conferences* **99** 01004
- [33] Kondratov A 2014 Thermo shrink films with interval macrostructure for protection of packaging from falsification *Modern Applied Science* **8** 204–9
- [34] Sittner P, Heller L, Pilch J and Curfs C 2014 Young's modulus of austenite and martensite phases in superelastic NiTi wires *J. Mat. Eng. Perf.* **23** 2059–2071
- [35] Novak V, Sittner P, Dayananda G, Fernandes M and Mahesh K 2008 On the electric resistance variation of NiTi and NiTiCu SMA wires in thermomechanical cyclic tests *Mater. Sci. Eng.* **481** 127–33
- [36] Panagopoulos C, Georgiou E, Giannakopoulos K and Orfanos P 2018 Effect of pH on stress corrosion cracking 6082 Al alloy *Metals.* **8** 578
- [37] Letaief W, Gamaon F and Hassine T 2017 Tensile behaviour of superelastic NiTi alloys charged with hydrogen under applied strain *Mater. Sci. Techn.* **33** 1533–1538